Cellulose (2021) 28:5761–5774
https://doi.org/10.1007/s10570-021-03911-w

ORIGINAL RESEARCH

Molybdenum disulphide/cellulose acetate nanofiber composite on screen printed electrodes for detecting cardiac troponin by electrical impedance spectroscopy

Kabhilan Gobalu · Mugashini Vasudevan · Subash C. B. Gopinath · Veeradasan Perumal · Mark Ovinis

Received: 19 January 2021 / Accepted: 4 May 2021 / Published online: 14 May 2021

Abstract Elevated levels of Troponin I, a cardiac biomarker, is indicative of an Acute Myocardial Infarction. However, current immunosensing methods to detect the presence of Troponin I such as Enzyme-Linked Immunosorbent Assay (ELISAs) has poor detection accuracy and unreliable quantitative results due to its single model readout. On the other hand, impedance spectroscopy detection using aptamer-modified electrodes is a more reliable and robust detection method, with higher sensitivity and better selectivity. In this paper, we propose a molybdenum disulphide/cellulose acetate (MoS_2/CA) nanofiber composite on screen printed electrodes for detecting troponin I by Electrical Impedance Spectroscopy. The MoS_2/CA nanofiber was electrospin at various amount of MoS_2 nanosheets (0.025 g, 0.05 g, 0.1 g and 0.2 g). Morphological, structural and optical characterization was conducted to discover the functional group as well as crystallinity formed in the MoS_2/CA composite nanofiber. The developed electrochemical nano-biosensor can detect up to 10 fM of Troponin I with 90% stability after 6 weeks, ~ 5 folds improvement compared to other proteins (selectivity), 0.89 μA mM^{-1} cm^{-2} sensitivity of sensor and RSD value of 3.8% (repeatability).

Keywords Troponin I · Molybdenum disulphide · Cellulose acetate · Nanofiber · Electrical impedance spectroscopy

Supplementary Information The online version contains supplementary material available at https://doi.org/10.1007/s10570-021-03911-w.

K. Gobalu · M. Vasudevan · V. Perumal · M. Ovinis
Centre of Innovative Nanostructures and Nanodevices (COINN), Universiti Teknologi PETRONAS, 32610 Seri Iskandar, Perak Darul Ridzuan, Malaysia

M. Vasudevan · V. Perumal (✉) · M. Ovinis
Department of Mechanical Engineering, Universiti Teknologi PETRONAS, 32610, Seri Iskandar, Perak Darul Ridzuan, Malaysia
e-mail: veeradasan.perumal@utp.edu.my

S. C. B. Gopinath
Institute of Nano Electronic Engineer, 01000 Kangar, Malaysia

S. C. B. Gopinath
School of Bioprocess Engineering, Universiti Malaysia Perlis, 02600 Arau, Perlis, Malaysia

Introduction

Cardiovascular diseases (CVDs) are the primary cause of death universally, with 31% of every death worldwide (~17.7 million deaths) in 2017 due to CVDs. Acute Myocardial Infarction (AMI), a CVD, can be diagnosed by the presence of elevated levels of Troponin I in the blood. Troponins are the protein fiber segments of the contractile cardiovascular and skeletal muscles, and are absent in smooth muscle. When a

patient has a heart attack or stroke, the troponin level in the blood increases.

Cardiac troponin complex has three subunits; Troponin I, which quells actin–myosin interchanges; Troponin C, which binds calcium and Troponin T, which joins the troponin complex and energizes narrowing. Enzyme-Linked Immunosorbent Assays (ELISAs) have been utilized for Troponin I and Troponin T detection and quantification (Cho et al. 2009). However, ELISA's is expensive and the assay procedure is tedious and laborious. Thus the need for a lower cost and process that is easy to automate (Perumal and Hashim 2014; Nezami et al. 2017). An obvious solution is the use of a nano biosensor. However, no commercially available nano-biosensor for the detection of a troponin is available in the market (Lee et al. 2019a).

Developing an efficient and effective nano biosensor requires nanoparticles that can sense the specific biomarker. Molybdenum Disulphide, MoS_2 has been widely used for its functionality, for example as a reactant hydride in the sulfurization of oil, for wear restriction and for nonaqueous lithium batteries. MoS_2 is a layered semiconductor (band hole = 1.2 eV, indirect) that withstands oxidation in moist air at temperatures of up to 85 °C (Nagaraju et al. 2007). This characteristic makes MoS_2 the nanomaterial of choice in the medical field. To further enhance its physical properties, many attempts have been made to develop MoS_2 nanomaterials.

MoS_2/CA nanofiber is formed by mixing MoS_2 nanosheet powder with cellulose acetate derivation (CA) and electrospinning the resulting mixture. Electrospinning has relative low cost, ease of use, is fast, supports many types of materials, and is adaptable, with the ability to control fiber arrangement, microstructure, and diameter (Teo and Ramakrishna 2009). Nanofiber-type cellulose acetate has it's a high surface to-mass ratio, high porosity with excellent pore interconnectivity and adaptability (Gopiraman et al. 2018).Cellulose acetate's chemical structure contains ether, hydroxyl and carboxyl, is ionic in nature and is ideal for binding metal nanoparticles to a polymer surface (Lee et al. 2005).

Materials and methods

Materials and reagents

Cellulose Acetate (Sigma 180955), N,N-Dimethylformamide (Merck 103053), Acetone (Merck 100014), Toluene (Merck 108325), Ethanolamine (Merck 822184), 16-mercaptohexadecanoic acid (Sigma 674435), 1 X Phosphate Buffered Saline (PBS) (BUF-2040-1 × 1L), (3-Aminopropyl) triethoxysilane (Sigma A3648), Hydrochloric acid 37% (Merck 822871), Molybdenum (VI) oxide (Sigma M0753), L-Cysteine (Merck 102838), N-(3-Dimethylaminopropyl)-N′-ethylcarbodiimide hydrochloric (Sigma E176), Acrylic acid N-hydroxysuccinimide ester (Sigma A8060). All of the chemicals were utilised as received without any extra purification steps. The oligonucleotides were purchased from Avantis Laboratory (Malaysia). The details of the oligonucleotide sequences utilized in this current work are as follows:

Oligo linker sequence of 5′-Biotin-C6-TTT TTT TTT TTT TTT TTT TT-3′.

Aptamer sequence of 5′- CGT GCA GTA CGC CAA CCT TTC TCA TGC GCT GCC CCT CTT AAA AAA AAA AAA AAA AAA AAA AAA A -3′; Target—Troponin I; Control—Troponin T; Human Serum from human male AB plasma purchased from Sigma-Aldrich Co., Ltd. (Malaysia).

Commercialized transducer Screen-Printed Electrode (SPE) was purchased from Metrohm DropSens (Malaysia).

Preparation of cellulose acetate (CA) solution

Preparation begins with 30 mL of Acetone poured into the beaker. Next, with the aid of pipette, 20 mL of dimethylformamide (DMF) added into the same beaker and the mixture stirred using magnetic stirrer with hot plate. Meanwhile stirring, 10.1 g of cellulose acetate powder weighed using precision weigh machine to get most accurate amount before the next procedure. After weighed, the cellulose acetate powder added into the solution in the beaker. Slowly the powder being added into the mixture to prevent coagulation of the powder inside the solution. The beaker covered with beaker cover lid to prevent contamination of the solution during stirring process. In order to ensure the cellulose acetate powder dissolve completely with the Acetone/DMF solution,

it stirred for 12 h, under room temperature and at 400 rpm (Lee et al. 2018).

Synthesizing molybdenum disulphide (MoS_2) nanosheet powder

The first procedure to fabricate MoS_2 nanosheet powder was having amount of 0.25 g of molybdenum (VI) oxide powder dissolving in 20 mL of distilled water where later proceeded with 20 min of sonication process by utilizing the sonication bath. Then, 50 mL of distilled water had been prepared as a dissolving medium for the 0.3 g L-cysteine. 100 mL beaker was prepared to accumulate the mixture solution after L-cysteine solution and molybdenum (VI) oxide solution mixed together in the beaker. In order to alter the pH of the mixture to pH 2.5, hydrochloric acid was utilized to serve mentioned purpose before pouring the solution into 250 mL Teflon—lined stainless steel autoclave. Right after the Teflon positioned in the oven, hydrothermal process carried out by applying the parameter of 16 h under 200 °C. Under room temperature the Teflon was left to cool down after completion of hydrothermal process for 16 h. After the cool down activity, black product obtained and washed three times continuously with ethanol and distilled water. Next, the black precipitate which was the MoS_2 nanosheet placed into crucible and dried at 45 °C for 8 h where afterwards it was transferred and stored inside a desiccator (Vasudevan et al. 2020).

Developing of MoS_2/CA solution

As this research studies the different mass of MoS_2 nanosheet powder reacting with the CA solution, the first experiment should be carried out with 0.025 g of MoS_2. After stirring the CA solution for 12 h, with the aid of precision weigh machine, the MoS_2 powder should be weighed to 0.025 g. Next, MoS_2 powder mixed into the CA solution in the same beaker and stirred for 1 h and under room temperature to ensure the MoS_2 disperse completely with the CA solution as existence of powder particles can cause blockage in tube during electrospinning process. Depends on the amount of MoS_2 being mixed with CA solution, the solution to be in the range of slight black to dark black as MoS_2 is in black in colour while CA solution normally colourless.

MoS_2/CA nanofiber via electrospinning

Electrospinning is the most convenient and cheapest method to produce MoS_2/CA. The interior of the electrospinning machine was first cleaned with an acetone solvent, and an aluminium foil which covered the drum used as a medium to collect the nanofiber. The feeding rate of the fibre is 0.4 mL/h with a fixed 15 cm distance between the needle and the drum, which rotates at a speed of 1200 rpm at a supply voltage of 10 V. After a 1 h stirring process, 20 mL of the MoS_2/CA solution was injected into the syringe. Electrospinning was performed for 8 h to obtain uniform nanofiber thickness and distribution. The specifications for the electrospinning machine were supply voltage fixed at 10 V, drum speed at 1200 rpm.

Surface functionalization

Screen-Printed Electrodes (SPE) were washed with 10 µL of 10 mM PBS at pH7.4 and the reading for bare SPE chips were subsequently taken to detect any manufacturing errors of the electrodes. The chips were incubated with 2% of aminopropyltriethoxysilane (APTES) for 1 h at room temperature. The chip was periodically check during the incubation process to ensure that the APTES was present on the chip. After 1 h of incubation, the unattached APTES was removed using 10 mM PBS of pH7.4. The pre-modified SPE chips with APTES were further enhanced by incubating with 10 µL r of 16-mercaptohexadecanoic acid mixed with N-hydroxysuccinimide (NHS) and ethylcarbodiimide (EDC) for 15 min. The 16-mercaptohexadecanoic acid powder was diluted with 250 µL of ethanol and 250 µL of water. The diluted 16-mercaptohexadecanoic acid was further mixed with 25 µL of NHS and 25 µL of EDC. The mixture was centrifuged for 2 min to produce white pellets for the electrode surface,

Next, the liquid form of MoS_2/CA nanofibers was prepared with 0.005 g of MoS_2/CA nanofiber and 5 mL of Toluene. The solution was sonicated for 80 min at 60 °C. The previous solution was added onto the modified SPE electrode, by letting the solution incubate for 30 min. The MoS_2/CA SPE electrodes were then modified by adding 10 µL of 1 Molar Streptavidin and incubated for 30 min. To block the unwanted Streptavidin/MoS_2/CA SPE structure, the electrodes were further modified by dropping 1 M of

ethanolamine as a blocking agent and incubated for 30 min. After each immobilisation steps, the SPE electrodes were washed with 10 µL of 10 mM PBS and impedance readings were taken (Gopinath et al. 2017).

Immobilisation and hybridisation of aptamer-biotin linker and target

The dilution of the probe is crucial before surface immobilization of the probe onto the electrode surface. For the biotin end of the linker to bind onto the streptavidin modified electrode surface, 973 µL of buffer solution was used to dilute the oligo linker sequence of 5′- /5Biosg//IC6Sp/TTT TTT TTT TTT TTT TTT TT-3′ which has 97.3 nM. For 100 µM of Aptamer with the sequence of 5′- CGT GCA GTA CGC CAA CCT TTC TCA TGC GCT GCC CCT CTT AAA AAA AAA AAA AAA AAA AAA AAA A -3′, which consists 62.3 nM, 623 µL of buffer solution was used for dilution. The biotin linkers were immobilised on the Streptavidin/MoS_2_CA/ SPE electrodes before immobilising the aptamer linker on the same modified electrodes, thus completing the probe (Biotin-Aptamer linker) immobilisation process. All washings were done with 10 µL of 100 mM PBS (pH 7.4) and readings were taken between each immobilization step.

For target detection, hybridization between the target (Troponin I) and probe was achieved by diluting Troponin I in 10 mM PBS of pH 7.4 at room temperature at different concentrations of troponin I ranging from 10 fM to 1 nM with the sequence of 10 fM, 100 fM, 1 pM, 10 pM, 100 pM and 1 nM, to obtain sequential data readings. Each target concentration dropped onto the electrode surface was incubated for 30 min and subsequently washed with 10 mM PBS of pH 7.4 before readings were taken. All steps are illustrated in Fig. 1a.

The steps were repeated using control protein (Troponin T) instead of Troponin I, with concentrations of 100 pM and 1 nM. Troponin T is the negative control protein to determine the detection sensitivity of the modified Aptamer /Streptavidin/MoS_2_CA/ SPE for different target besides Troponin I.

Microscopic-nanoscale imaging

Field-emission scanning electron microscopy (FESEM; Carl Zeiss AG ULTRA55, Gemini) used to investigate the morphology and structural properties of MoS_2/CA nanofiber samples. Transmission Electron Microscope (TEM) were used to analyse the image in nanoscale level. HITACHI HT 7830 series up to 120 kV used to carry out high resolution TEM (HRTEM) images of MoS_2/CA nanofiber. Preparation of the sample carried out by dispersing the MoS_2/CA nanofiber in toluene and sonicated for one hour.

Structural analysis

Crystallization and structural properties of MoS_2/CA nanofiber analysed with X-ray diffraction (XRD, Bruker D8, Bruker AXS, Inc., Madison, WI, USA. The X-ray diffraction (XRD) pattern was recorded in the range of 30° to 60° operating at a voltage of 40 kV and a current of 40 mA. The X-ray spectra peak analysis was carried out by Diffraction plus 2003 version of Eva 9.0 rev.0 software.

Impedance spectroscopy

Impedance spectroscopy readings were obtained by utilizing NOVA control alpha high-frequency analyser (Hundsangen, Germany). To describe the MoS_2/CA nanofiber, arranged example was drenched in PBS (pH 7.4) containing a blend of 2 mM K3[Fe(CN)6]/K4[Fe(CN)6]. Zs' and Zs'', where reflect onto real and imaginary parts were acquired by clearing the frequency of 1–100 MHz with an applied AC adequacy of 1 V RMS. Every one of the readings and measurement were done at room temperature.

Optical measurements

The consumed chemical exacerbates that left on the surface of MoS_2/CA nanofiber was created on SiO2/Si substrate were distinguished utilizing the Fourier transform infrared spectroscopy (FTIR, PerkinElmer Spectrum 400 spectrometer, PerkinElmer, Waltham, MA, USA).

Results and discussion

MoS_2/CA nanofiber morphology analysis

The morphology structure of all samples were studied through FESEM. For the 0.025 g of MoS_2 nanosheet

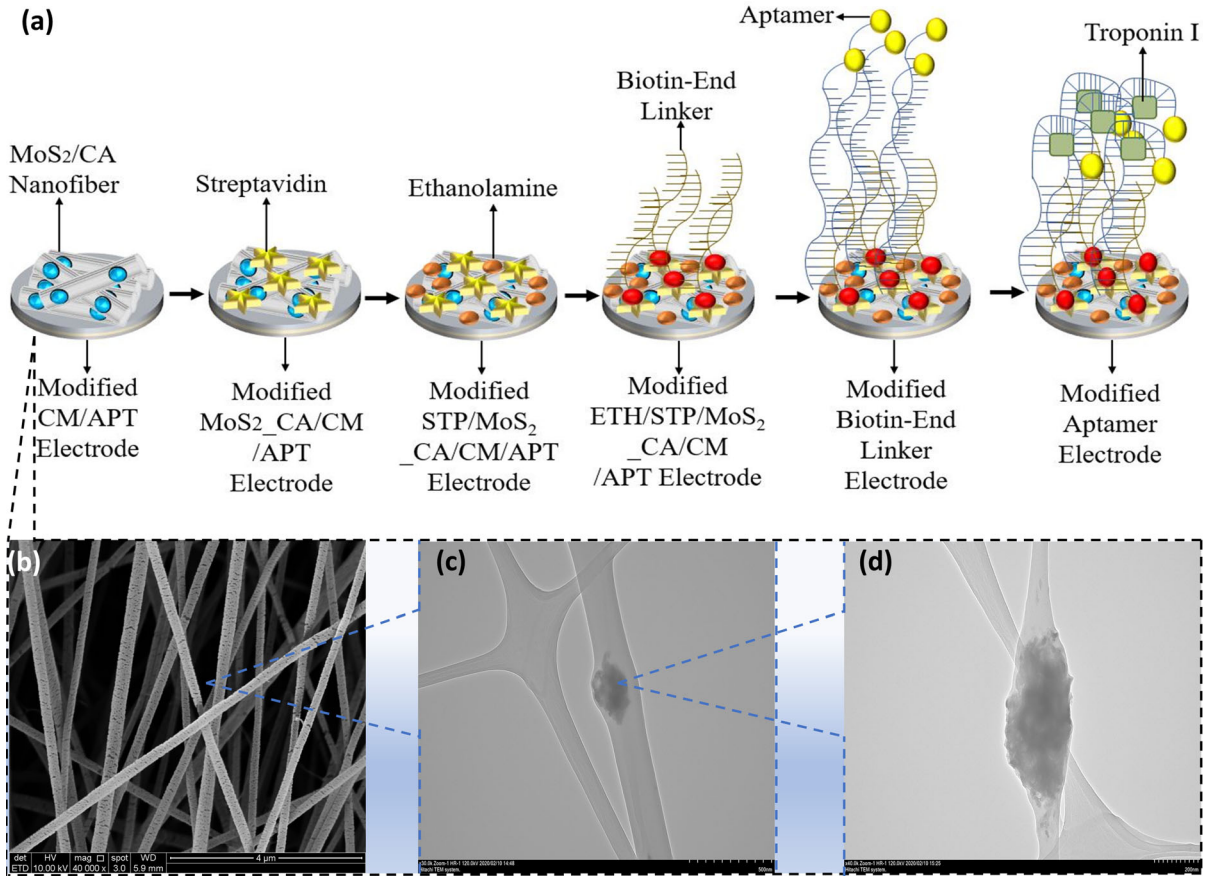

Fig. 1 **a** Schematic illustration of surface functionalization processes from bare electrode until aptamer immobilization and target detection. **b** FESEM image of low magnification revealing smooth surface nanofiber structure of MoS_2 dispersed. **c**, **d** Low- and high-magnification TEM images of MoS_2 nanosheet successfully dispersed into CA nanofiber

with CA, as shown in Fig. 2a, the surface of the nanofiber is smooth with less spores observed. The diameter of each nanofiber is not similar in size with a randomly oriented network structure and a beads-free structure, as there is no undissolved MoS_2 nanoparticles (Huang et al. 2003). The MoS_2/CA is a homogenous solution, as the MoS_2 nanosheet powder was completely dispersed (Liu et al. 2015). The nanofibers are stacked layer by layer, as shown by the different colour concentration of nanofibers, where at upper layers brighter and the bottom layers darker. As shown in Fig. 2b,c, the nanofibers formed exhibits a similar structure with the nanofibers in Fig. 2a, with the only difference being the diameters of the nanofibers. Thus, it can be concluded that more nanofibers can be produced by adding more MoS_2 nanosheet powder into the solution. However, the amount of MoS_2 nanosheet powder that can be added into the solution to produce MoS_2/CA nanofibers has a limit. As shown in Fig. 2d, there is coiling of small diameter nanofibers onto another nanofiber. This phenomenon, known as micro-coiling, is a common phenomenon when using electrospinning to produce nanofiber, due to bending instability. Micro-coiling can be seen when the amount of MoS_2 increases when mixed with a fixed amount CA, compared with previous samples which do not exhibit any coiling. Viscosity plays a vital role in contributing to bending instability (Yarin et al. 2001). The viscosity of a sample increases due to increasing amount of MoS_2 added, as it makes the solution more concentrated. As the amount of MoS_2 is increased, more micro-coiling is observed, as shown in Fig. 2d. Thus, a maximum of 0.2 g of MoS_2 nanosheet powder is recommended to avoid micro-coiling, as this phenomenon disrupts the mechanical and physical properties of MoS_2/CA nanofiber and makes the

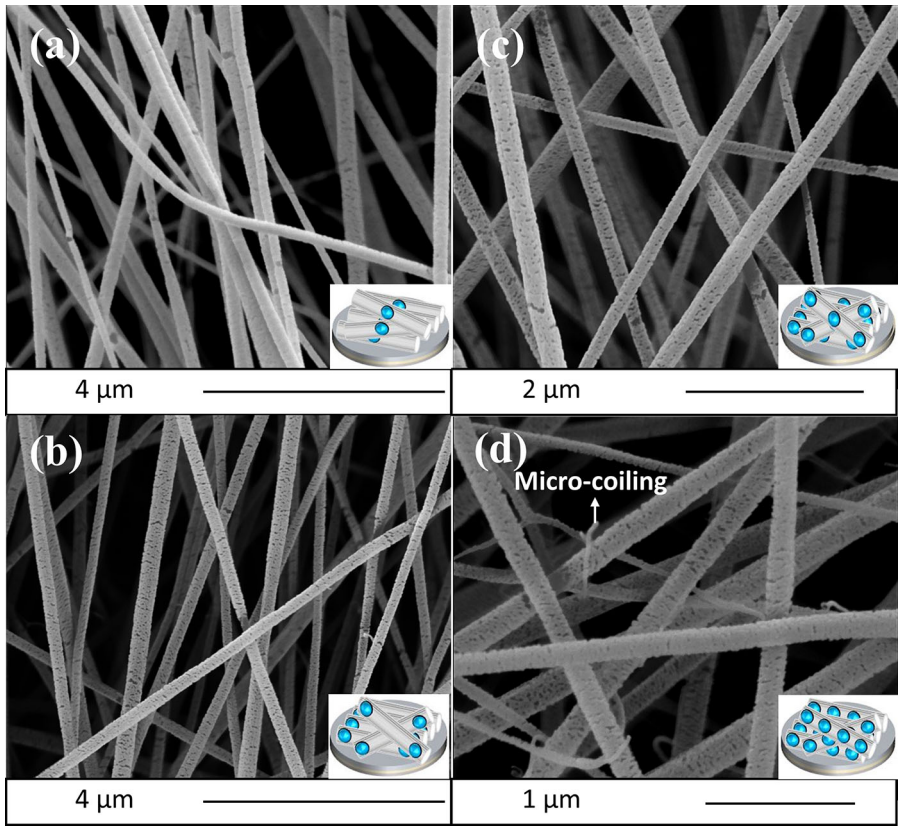

Fig. 2 FESEM image on morphology structure of **a** 0.025 g MoS_2/CA nanofiber, **b** 0.05 g MoS_2/CA nanofiber, **c** 0.1 g MoS_2/CA nanofiber, **d** 0.2 g MoS_2/CA nanofiber

surface functionalization process more complex. As such, only the 0.025 g, 0.05 and 0.1 g of MoS_2/CA samples were used, as the 0.2 g MoS_2/CA exhibited poor nanofiber structure due to presences of micro-coiling that can obstruct biomolecules from binding on the surface of the biosensor. In conclusion, we devised to carry our further analysis using 0.05 g of MoS2/CA sample as the morphology structure resembles an optimum structure for a nanofiber and suitable for other characterization processes.

The MoS_2/CA-0.05 nanofiber (0.05 g MoS_2 nanosheet) morphology was analyzed using Transmission Electron Microscope (TEM). As observed in Fig. 1c,d, the MoS_2 nanosheet is embedded with nanofibers. This demonstrates that the MoS_2 nanosheets are highly dispersed within the cellulose acetate nanofibers. This structural feature is an advantage for increasing surface area per volume ratio (Chen et al. 2019). For more TEM figures, please refer to Supplementary Fig. 1.

Fourier transform-infrared (FT-IR) spectroscopy

FTIR spectroscopy was performed to determine the functional group or elements present based on their vibrational characteristic. The peak observed at 606 cm^{-1} in Fig. 3a corresponds to the Mo–S bond shifting from its original spectra value, which is 469 cm^{-1}, due to mixture reaction of MoS_2 with CA, with electrons/synergistic interaction occurring at a molecular level (Zhao et al. 2013; Sudiarti et al. 2017; Ahmad et al. 2020). The peak at 1036 cm^{-1} is due to the vibration of sulphur from MoS_2 together with oxygen from CA, from the S–O bond (Feng et al. 2013). The absorption peak at 906 cm^{-1} is attributed to the stretching of S–S present in MoS_2. The presence of CA can be proven by the presence of the C–O–C and C=O bonds, observed at 1234 cm^{-1} and 1758 cm^{-1} respectively (Song et al. 2012). The –CH2 deformation vibration at 1372 cm^{-1} for pure cellulose acetate has been shifted to 1369 cm^{-1} for MoS_2/CA. The peak FTIR spectras values for pure cellulose acetate and MoS_2 nanosheet are shown in Fig. 3b, c respectively. The wavenumber

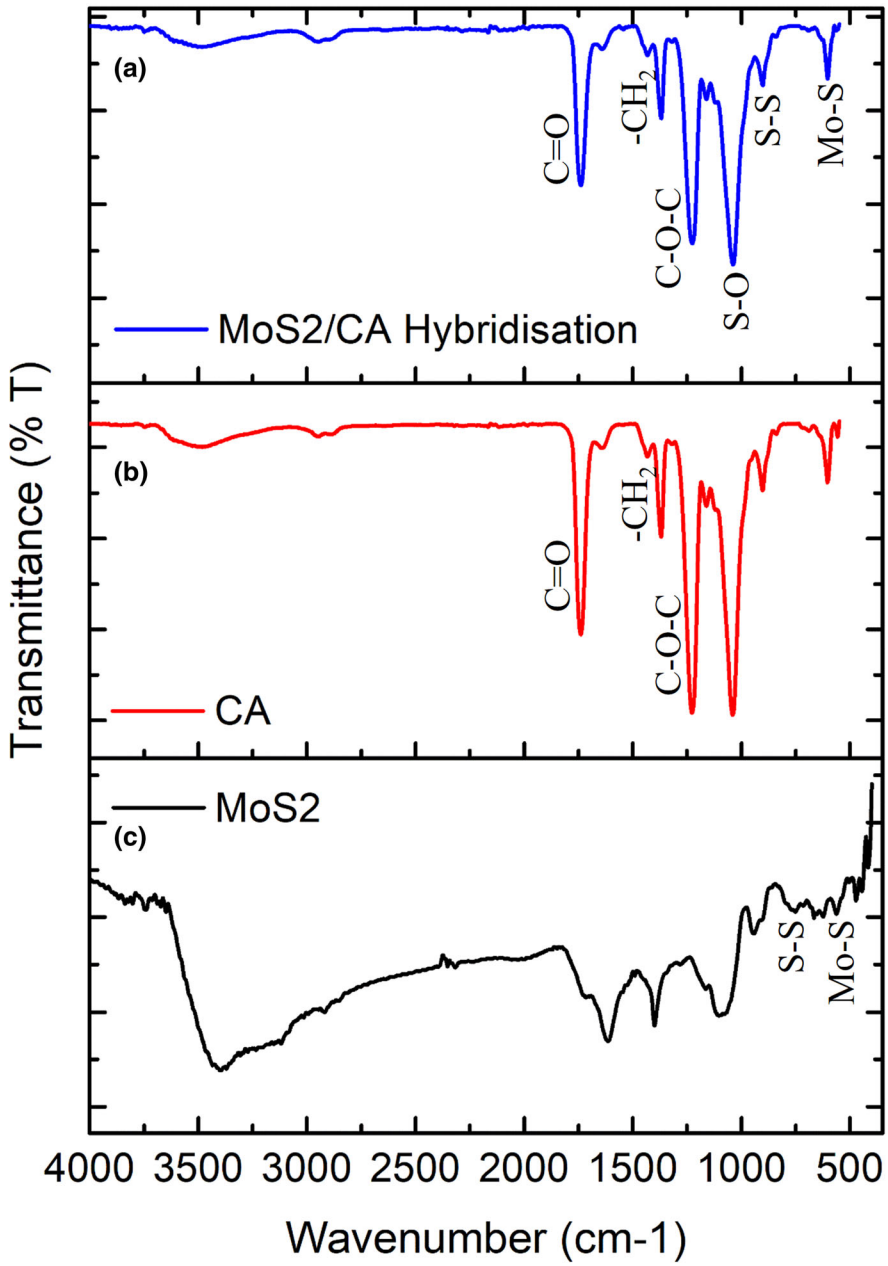

Fig. 3 FT-IR spectrum **a** MoS_2/CA nanofiber hybridisation, **b** pure cellulose acetate, **c** MoS_2 nanosheet

obtained for each peak of functional group present in MoS_2/CA hybridization had exhibited almost similar wavenumber of the cellulose acetate FTIR spectra and MoS_2 nanosheet FTIR spectra, proving the presence of CA and MoS_2 nanosheet in the MoS_2/CA nanofiber hybridization.

X-ray diffraction (XRD)

As shown in XRD spectrum in Fig. 4a, it can be deduced that the sample is in amorphous form, as there is no clear diffraction peak observed on the XRD spectrum (Yu and Park 2016). However, there is diffraction at peak of 15° in the XRD spectrum from the MoS_2/CA nanofiber hybridisation, which

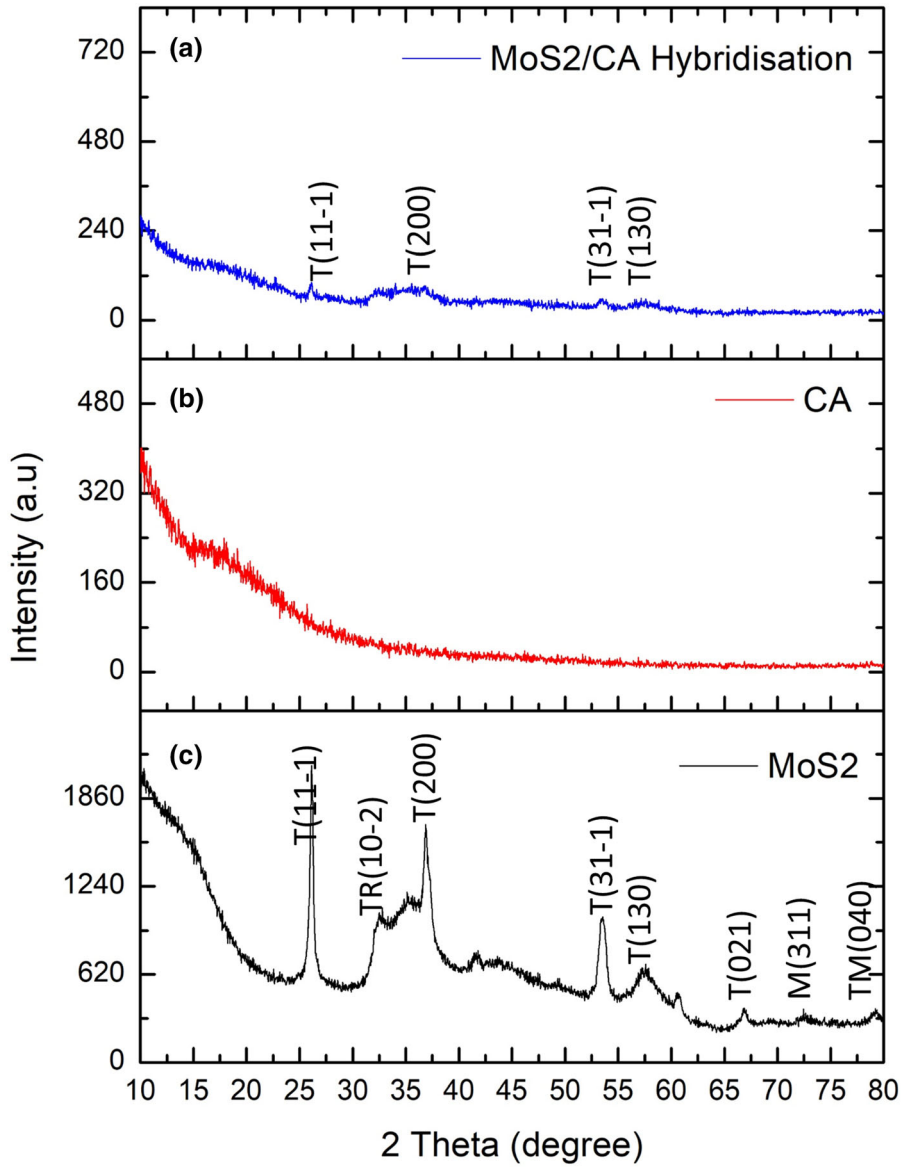

Fig. 4 XRD spectrum **a** MoS_2/CA nanofiber hybridisation, **b** pure cellulose acetate, **c** MoS_2 nanosheet

resembles the diffraction of the cellulose acetate spectrum, indicating the presence of cellulose acetate in the hybridisation. From Fig. 4c, the diffraction peaks found at 26.1°, 32.8°, 36.9°, 53.5°, 60.6°, 66.9°, 72.9° and 79.5° reflecting onto the T(11 −1), TR(10 − 2), T(200), T(31 −1), T(130), TM(021), M(311) and TM(040) planes resembles the XRD spectrum of the MoS_2 nanosheet only (Vasudevan et al. 2020). In Fig. 4a, the spectrum exhibited some of the same diffraction peaks with XRD spectrum obtained in Fig. 4b and c, such as the T(11 −1), T(200), T(31 −1) and T(130) planes, indicating the presence of MoS_2 nanosheet in MoS_2/CA nanofiber hybridisation. The reason behind the shape of peak diffraction at the same degree in the hybridisation compared to MoS_2 nanosheet diffraction, is because the MoS_2 nanosheet were dispersed and layered into the CA nanofiber, as can be observed in morphology analysis earlier.

Impedance measurement for MoS_2/CA composite

EIS was carried out to investigate the electrochemical process at various doping amount of MoS_2 nanosheets in CA polymer solution forming MoS_2/CA composite nanofiber and further analyze the impedance spectroscopy on the surface modified SPE electrode at room temperature as shown in Supplementary Fig. 2. The interception of the semicircle with the X-axis in high-frequency regions represents the equivalent series resistance (Rs) of the electrode materials, whereas the diameter of the semicircle corresponds to the resistance of the transfer of charge (Rct) due to redox reaction. At low impedance frequency regions, the line axis that is almost parallel to the imaginary shows that 0.05 g of MoS_2/CA composite has an ideal capacitive behavior and lower transfer resistances. Furthermore, the variation in semicircle for all the compositions indicates the non-Debye nature and the distribution of the relaxation time (Ali et al. 2013; Monisha et al. 2016; Shanmuga Priya et al. 2018). 0.05 g of MoS_2/CA composite displayed the lowest Rct and impedance value compared to other concentrations. The result also revealed that addition of 0.05 g of MoS_2 in CA polymer gives high ionic conductivity as the number of charge carries increase (Mahalakshmi et al. 2019). The number of charge carries rises in such a way that the sulfide salt dissociate into Mo^{2+} and S^{2-} ions, due to that more charge carries is formed. Thus, the maximum number of charge carriers is formed in 0.05 g of MoS_2/CA composite which also leads to faster charge transfer rates and higher flexibility of the polymer chain for intercalation. Besides that, addition of lower or higher amount of MoS_2 than 0.05 g in composite, decreases the conductivity which directly affects the aggregation of ions in polymer network. The results indicated improvement in storage and transport of charges within the electrode attributed highly by 0.05 g of MoS_2/CA composite compared to other concentration. At low frequencies, the 0.05 g of MoS_2/CA composite had pure capacitive behaviors as that composite demonstrates nearly vertical straight line (Wang et al. 2015). Hence, the 0.05 g of MoS_2/CA composite has been used to further elucidate the biosensing capacity via impedance spectroscopy analysis.

Impedance measurement for surface functionalization

Before detection of the target, the surface functionalization was verified by analysing its impedance spectra using Electrical Impedance Spectroscopy (EIS). Specifically, the Rct, Ra and CPE of a Randles equivalent circuit, where Rct is the charge transfer resistance, Ra is the bulk solution resistance and CPE is for constant phase element, were determined. From the EIS, the semicircles of a Nyquist plot, as shown in Fig. 5a, corresponds to the charge transfer resistance, Rct. The increase in Rct was due to the expansion in charge transfer resistance. The changes of each semicircle diameter in Fig. 5a indicates the changes in electrical properties of the modified electrode surface upon each immobilization step. The MoS_2/CA nanofiber immobilization has the lowest impedance reading, with a peak value of 948 Ω. With immobilization of streptavidin, the peak value increases to 1335 Ω, indicating the streptavidin has successfully immobilized on the MoS_2/CA modified electrode. The charge transfer resistance of the surface increases due to existence of protein molecules in Streptavidin, causing the surface to be less conductive, thus increasing resistance. A further increment of impedance of 1774 Ω was obtained when Ethanolamine, a blocking agent, was dropped onto the modified surface. The impedance increased due to ethanolamine blocking target binding onto the surface and onto streptavidin instead. As for the aptamer with biotin-linker added onto the modified electrode, the impedance spectrum is almost similar to streptavidin's impedance spectra, but with slightly higher value of impedance of 1382 Ω. This prove that rather than binding onto the surface, the aptamer-biotin linker had bound completely to the streptavidin binding sites, hence exhibiting almost similar electrical characteristics with the impedance spectrum of streptavidin. Moreover, it also proves that ethanolamine, as blocking agent, had prevented bio-fouling i.e. binding of the aptamer-biotin linker onto the non-streptavidin covered electrode surface.

Detection of Troponin I

Having achieved surface functionalization by the immobilization of aptamer, the electrode was further analysed to determine the detection limit. Various

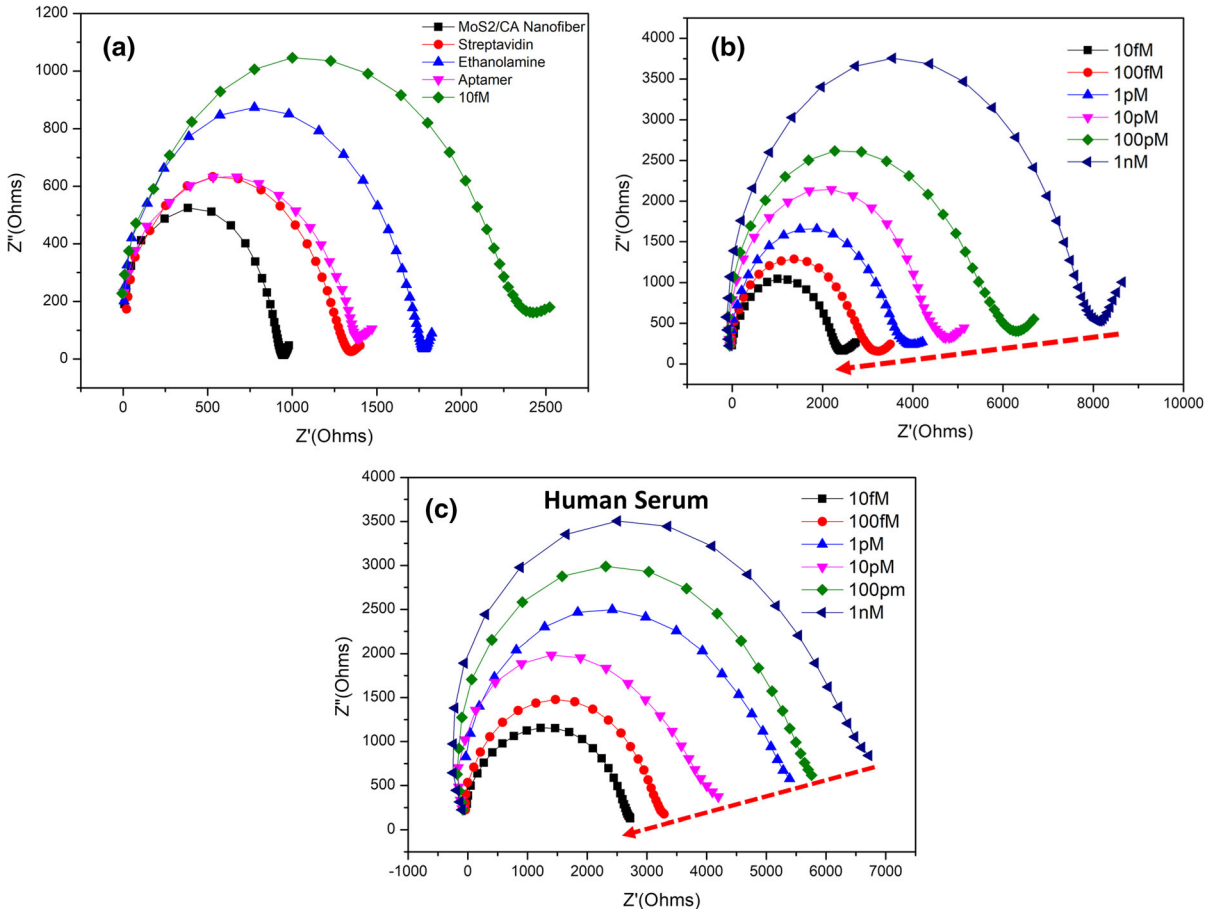

Fig. 5 **a** Impedance spectra of each steps done in surface functionalization procedure to study the electrical properties and charge transfer resistance to determine the immobilization succeed or failure. **b** Impedance analysis for the interaction aptamer and target with different concentration. The impedance spectra of the real and imaginary parts of impedance, Zs′ and Zs″, were plotted using Nyquist plot. The target concentration detected with range of 10fM to 1nM. **c** Impedance analysis for the interaction aptamer and human serum with different concentration. The impedance spectra of the real and imaginary parts of impedance, Zs′ and Zs″, were plotted using Nyquist plot. The human serum concentration detected with range of 10 fM to 1 nM

Troponin I concentrations (10 fM–1 nM) was applied onto the aptamer modified electrode and measured by EIS. As shown in Fig. 5b, the charge transfer resistance increases with increasing concentrations of Troponin I hybridized on the modified electrode. The lowest concentration of Troponin I, 10 fM, recorded an impedance value of 2423 Ω and the 100 fM concentration of Troponin I had an impedance value of 3163 Ω. The impedance for 1 pM, 10 pM, 100 pM and 1 nM are 3805 Ω, 4801 Ω, 6220 Ω and 8131 Ω respectively. The Rct value increases significantly as the concentration increases because the number of binding sites increases on the surface of the electrode due to the increase of negative charge ions in proteins and an increment in the surface coverage of Troponin I (Wang et al. 2016).

Troponin I detection in human serum

Figure 5c shows the EIS readings for the detection of Troponin I in human serum to assess the sensitivity of the modified electrode to detect Troponin I when mixed with other proteins in the human serum. The charge transfer resistance increases as the human serum concentration increase. The sensor successfully detected Troponin I as only the specified protein captured by aptamer on the electrode. Therefore, the

modified aptamer-biotin linker acts as a biological recognition molecule to specifically detect Troponin I.

High analytical performance sensor

The biosensor can detect Troponin I in concentrations as low as 10 fM (1×10^{-14} M). As shown in Fig. 6a, the linear regression, R^2, has a value of 0.96022 indicating good linear relationship between sensitivity and increment of Troponin I concentration. The sensitivity is (Balakrishnan et al. 2014; Vasudevan et al. 2021):

$$\text{Sensitivity} = \frac{\text{Slope of calibration plot, m}\left(\mu\text{A mM}^{-1}\right)}{\text{Active Surface Area, A}\left(\text{cm}^2\right)}$$

The active surface area of SPE, A = 0.1257 cm^2 and the sensitivity of the sensor is 0.894 μA mM^{-1} cm^{-2}. The sensitivity or detection limit of this biosensor is better compared to other Tropinin I biosensors, with 90% more sensitivity than a recently developed sensor with a detection limit of 110 fM (Lee et al. 2019b). Table 1 shows the comparison of limit of detection among the currently available researches on detection of Troponin I.

To determine the selectivity of the biomolecules detection, different combinations were used, such as control (Troponin T), other proteins and human serum.

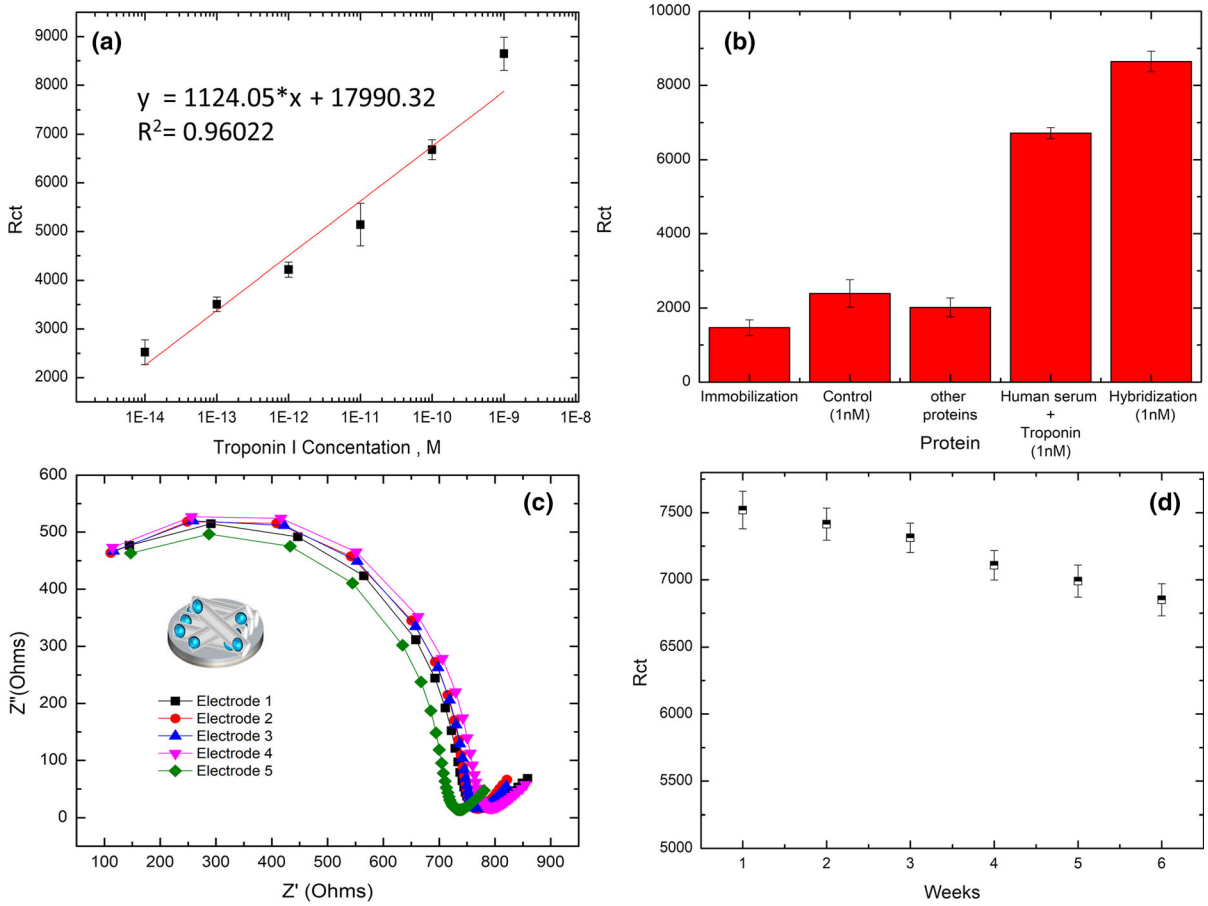

Fig. 6 **a** Linear regression analysis to determine the linearity of detection based on different concentration of target. Mean data from different electrodes were calculated and plotted. R2 value implies the significance. **b** The bar diagram shows selectivity of the SPE sensor towards detection of Troponin I and other proteins in form of human serum and control (Troponin T). **c** Repeatability analysis on five different electrodes under same processes. **d** Stability analysis throughout 6 weeks continuously to determine the performance rate and durability of the developed sensor

Table 1 Comparison of the currently available detection of Troponin I

Method	Strategy	Limit of Detection	References
Immunosensor	A functionalized SnO2 nanobelt field-effect transistors (FETs) with integrated microfluidics	100 pM	Cheng et al. (2011)
Immunosensor	Silicon nanowire FET-based biosensor	5 pM	Kim et al. (2016)
Aptasensor	DNA aptamers against Troponin I were identified by the Systematic Evolution of Ligands by Exponential enrichment (SELEX) method	1 pM	Jo et al. (2015)
Aptasensor	A sandwich aptamer-based screen-printed carbon electrode (SPCE) using chronoamperometry	1 pM	Jo et al. (2017)
Aptasensor	Multi-functional DNA (MF-DNA) on Au nanocrystal (AuNC) using an electrochemical method (EC) and a localized surface plasmon resonance (LSPR) method	110 fM	Lee et al. (2019b)
Aptasensor	SPE modified with Molybdenum Disulphide/Cellulose Acetate nanofiber and detection using EIS	10 fM	This work

Figure 6b shows the Rct value for each type of combination immobilized on the electrode. The charge transfer resistance does not significantly change or differ when unrelated molecules such as the control and other protein were introduced. The Rct values are almost the same Rct value of the immobilized electrode, meaning the sensor does not detect unrelated biomolecules, as the aptamer was modified to capture Troponin I proteins only. For Troponin I with human serum, the Rct readings where higher when compared to the control and other protein concentration. The aptamer-biotin linker can therefore be functionalized on the electrode surface to capture and detect Troponin I proteins only.

The repeatability was checked by analysing the impedance spectrum for SPE electrodes used for target concentration, human serum and control detection. As shown in Fig. 6c, the impedance spectra of all electrodes used after MoS_2/CA nanofiber immobilization on electrode surfaces showed almost similar impedance spectrum with no significant differences. The sensing system of each electrode used in this experiment with immobilisation of MoS_2/CA nanofiber has therefore high sensitivity and specificity. The immobilized electrode was tested from 1st week to 6th week, to ensure it was robust and reliable. Based on Fig. 6d, the functionality declined slightly over the weeks, with a performance percentage rate of 90%.

Conclusions

In this research, a highly selective and sensitive nano biosensor using Screen-Printed Electrodes (SPE) and EIS was developed for the detection of Troponin I. The advantage of this sensor includes its high sensitivity, low detection limit for low concentrations of Troponin I (target), great stable surface and remarkable specificity. The higher surface capture ability is due to the MoS_2/CA nanofiber, which immobilized beneath aptamer, facilitated target hybridization. Even in the presence of human serum, the results obtained from the detection shows a significant increment in the sensitivity of sensor, with a detection limit of up to 10 fM with RSD value of 3.8% and $\sim$ 5 folds selectivity. This study has shown promising results and may possibly be extended for the detection of other biomarkers.

Acknowledgments The authors would like to thank Universiti Teknologi PETRONAS (UTP) for the financial support through URIF-Grant (015LBO-021). The appreciation also goes to all the team members and staffs in the Department of Mechanical Engineering UTP and Centre of Innovative Nanostructure and Nanodevices (COINN).

Author Contributions K.G and V.P conceived and developed the new Molybdenum Disulphide/Cellulose Acetate nanofiber. K.G and M.V carried out the experiment and drafted the manuscript. S.C.B.G, M.O and V.P proofread the manuscript. V.P supervised the work. All authors analysed the results and contributed to the discussion presented in the manuscript.

Funding Universiti Teknologi PETRONAS (UTP) for the financial support through URIF-Grant (015LBO-021).

Data availability Correspondence and requests for data that support the findings of this study should be addressed to V.P upon request.

Code availability Not applicable.

Declarations

Conflict of interest The authors declare that they have no known conflict of interests or personal relationships that could have appeared to influence the work reported in this paper. Supplementary information accompanies this paper attached together during submission.

Ethical approval This study does not involve any animal and human sample.

References

Ahmad S, Khan I, Husain A et al (2020) Electrical conductivity based ammonia sensing properties of polypyrrole/MoS2 nanocomposite. Polymers. https://doi.org/10.3390/polym12123047

Ali R, Harun NI, Malik A et al (2013) Effect of temperature on conductivity studies of cellulose acetate based polymer electrolytes. 667:240–245. https://doi.org/10.4028/www.scientific.net/AMR.667.240

Balakrishnan SR, Hashim U, Letchumanan GR et al (2014) Development of highly sensitive polysilicon nanogap with APTES/GOx based lab-on-chip biosensor to determine low levels of salivary glucose. Sens Actuators A 220:101–111. https://doi.org/10.1016/j.sna.2014.09.027

Chen H, He J, Ke G et al (2019) MoS2 nanoflowers encapsulated into carbon nanofibers containing amorphous SnO2 as an anode for lithium-ion batteries. Nanoscale 11:16253–16261. https://doi.org/10.1039/c9nr05631a

Cheng Y, Chen KS, Meyer NL et al (2011) Functionalized SnO 2 nanobelt field-effect transistor sensors for label-free detection of cardiac troponin. Biosens Bioelectron 26:4538–4544. https://doi.org/10.1016/j.bios.2011.05.019

Cho IH, Paek EH, Kim YK et al (2009) Chemiluminometric enzyme-linked immunosorbent assays (ELISA)-on-a-chip biosensor based on cross-flow chromatography. Anal Chim Acta 632:247–255. https://doi.org/10.1016/j.aca.2008.11.019

Feng X, Tang Q, Zhou J et al (2013) Novel mixed-solvothermal synthesis of MoS2 nanosheets with controllable morphologies. Cryst Res Technol 48:363–368. https://doi.org/10.1002/crat.201300003

Gopinath SCB, Perumal V, Balakrishnan SR et al (2017) Aptamer-based determination of ATP by using a functionalized impedimetric nanosensor and mediation by a triangular junction transducer. Microchim Acta 184:4425–4431. https://doi.org/10.1007/s00604-017-2485-8

Gopiraman M, Deng D, Saravanamoorthy S et al (2018) Gold, silver and nickel nanoparticle anchored cellulose nanofiber composites as highly active catalysts for the rapid and selective reduction of nitrophenols in water. RSC Adv 8:3014–3023. https://doi.org/10.1039/c7ra10489h

Huang ZM, Zhang YZ, Kotaki M, Ramakrishna S (2003) A review on polymer nanofibers by electrospinning and their applications in nanocomposites. Compos Sci Technol 63:2223–2253. https://doi.org/10.1016/S0266-3538(03)00178-7

Jo H, Gu H, Jeon W et al (2015) Electrochemical aptasensor of cardiac troponin i for the early diagnosis of acute myocardial infarction. Anal Chem 87:9869–9875. https://doi.org/10.1021/acs.analchem.5b02312

Jo H, Her J, Lee H et al (2017) Highly sensitive amperometric detection of cardiac troponin I using sandwich aptamers and screen-printed carbon electrodes. Talanta 165:442–448

Kim K, Park C, Kwon D et al (2016) Silicon nanowire biosensors for detection of cardiac troponin I (cTnI) with high sensitivity. Biosens Bioelectron 77:695–701

Lee JH, Lee LH, Nam J, Do et al (2005) Water uptake and migration effects of electroactive ion-exchange polymer metal composite (IPMC) actuator. Sens Actuators A 118:98–106. https://doi.org/10.1016/j.sna.2004.07.001

Lee H, Nishino M, Sohn D et al (2018) Control of the morphology of cellulose acetate nanofibers via electrospinning. Cellulose 25:2829–2837. https://doi.org/10.1007/s10570-018-1744-0

Lee T, Ahn JH, Choi J et al (2019a) Development of the troponin detection system based on the nanostructure. Micromachines. https://doi.org/10.3390/mi10030203

Lee T, Kim J, Nam I et al (2019b) Fabrication of troponin i biosensor composed of multi-functional dna structure/au nanocrystal using electrochemical and localized surface plasmon resonance dual-detection method. Nanomaterials. https://doi.org/10.3390/nano9071000

Liu C, Wang L, Tang Y et al (2015) Vertical single or few-layer MoS2 nanosheets rooting into TiO2 nanofibers for highly efficient photocatalytic hydrogen evolution. Appl Catal B 164:1–9. https://doi.org/10.1016/j.apcatb.2014.08.046

Mahalakshmi M, Selvanayagam S, Selvasekarapandian S, Moniha V (2019) Characterization of biopolymer electrolytes based on cellulose acetate with magnesium perchlorate (Mg (ClO 4) 2) for energy storage devices. J Sci Adv Mater Dev 4:276–284. https://doi.org/10.1016/j.jsamd.2019.04.006

Monisha S, Mathavan T, Selvasekarapandian S, Benial AMF (2016) Preparation and characterization of cellulose acetate and lithium nitrate for advanced electrochemical devices. Ionics. https://doi.org/10.1007/s11581-016-1886-8

Nagaraju G, Tharamani CN, Chandrappa GT, Livage J (2007) Hydrothermal synthesis of amorphous MoS 2 nanofiber bundles via acidification of ammonium heptamolybdate tetrahydrate. Nanoscale Res Lett 2:461–468. https://doi.org/10.1007/s11671-007-9087-z

Nezami A, Nosrati R, Golichenari B et al (2017) Nanomaterial-based aptasensors and bioaffinity sensors for quantitative

detection of 17β-estradiol. TrAC Trends Anal Chem 94:95–105. https://doi.org/10.1016/j.trac.2017.07.003

Perumal V, Hashim U (2014) Advances in biosensors: principle, architecture and applications. J Appl Biomed 12:1–15. https://doi.org/10.1016/j.jab.2013.02.001

Shanmuga Priya S, Karthika M, Selvasekarapandian S et al (2018) Study of biopolymer I-carrageenan with magnesium perchlorate. Ionics 24:3861–3875. https://doi.org/10.1007/s11581-018-2535-1

Song J, Birbach NL, Hinestroza JP (2012) Deposition of silver nanoparticles on cellulosic fibers via stabilization of carboxymethyl groups. Cellulose 19:411–424. https://doi.org/10.1007/s10570-011-9647-3

Sudiarti T, Wahyuningrum D, Bundjali B, Made Arcana I (2017) Mechanical strength and ionic conductivity of polymer electrolyte membranes prepared from cellulose acetate-lithium perchlorate. IOP Conf Ser Mater Sci Eng https://doi.org/10.1088/1757-899X/223/1/012052

Teo WE, Ramakrishna S (2009) Electrospun nanofibers as a platform for multifunctional, hierarchically organized nanocomposite. Compos Sci Technol 69:1804–1817. https://doi.org/10.1016/j.compscitech.2009.04.015

Vasudevan M, Tai MJY, Perumal V et al (2020) Highly sensitive and selective acute myocardial infarction detection using aptamer-tethered MoS2 nanoflower and screen-printed electrodes. Biotechnol Appl Biochem https://doi.org/10.1002/bab.2060

Vasudevan M, Tai MJY, Perumal V et al (2021) Cellulose acetate-MoS2 nanopetal hybrid: a highly sensitive and selective electrochemical aptasensor of Troponin I for the early diagnosis of Acute Myocardial Infarction. J Taiwan Inst Chem Eng 118:245–253. https://doi.org/10.1016/j.jtice.2021.01.016

Wang J, Wu Z, Hu K et al (2015) High conductivity graphene-like MoS 2/polyaniline nanocomposites and its application in supercapacitor. J Alloys Compd 619:38–43. https://doi.org/10.1016/j.jallcom.2014.09.008

Wang B, Jing R, Qi H et al (2016) Label-free electrochemical impedance peptide-based biosensor for the detection of cardiac troponin I incorporating gold nanoparticles modified carbon electrode. J Electroanal Chem 781:212–217. https://doi.org/10.1016/j.jelechem.2016.08.005

Yarin AL, Koombhongse S, Reneker DH (2001) Bending instability in electrospinning of nanofibers. J Appl Phys 89:3018–3026. https://doi.org/10.1063/1.1333035

Yu X, Park HS (2016) Synthesis and characterization of electrospun PAN/2D MoS2 composite nanofibers. J Ind Eng Chem 34:61–65. https://doi.org/10.1016/j.jiec.2015.10.030

Zhao J, Zhang Z, Yang S et al (2013) Facile synthesis of MoS2 nanosheet-silver nanoparticles composite for surface enhanced Raman scattering and electrochemical activity. J Alloy Compd 559:87–91. https://doi.org/10.1016/j.jallcom.2013.01.067